Algorithm and validation of a tropical cyclone central pressure estimation method based on warm core intensity as observed using the Advanced Microwave Sounding Unit-A (AMSU-A)

Ryo Oyama
Meteorological Research Institute, Japan Meteorological Agency

Abstract

The Meteorological Research Institute (MRI) of the Japan Meteorological Agency (JMA) developed a new method for estimating tropical cyclone (TC) minimum sea level pressure (MSLP) from TC warm core intensity as observed using the Advanced Microwave Sounding Unit-A (AMSU-A). This approach is based on regression between TC warm core intensity data obtained from AMSU-A 55-GHz band brightness temperatures and MSLP values in best-track data archived by the Regional Specialized Meteorological Center (RSMC) Tokyo - Typhoon Center for TCs in the western North Pacific basin during the 2008 TC season. The root mean square error and bias of MSLP values estimated using the new method with reference to best-track data for TCs observed in 2009–2011 were 10.1 hPa and 0.3 hPa, respectively. Based on several TCs as examples, this paper also explains the characteristic aspects of MSLP values estimated by the new method in relation to TC cloud pattern and TC size.

1. Introduction

The estimation of tropical cyclone (TC) intensity is important for disaster prevention and mitigation. In general, minimum sea level pressure (MSLP) or maximum sustained wind is used as a scale of TC intensity. Within the Japan Meteorological Agency (JMA), MSLP estimates from the results of monitoring efforts such as in situ and satellite observation have been used to create a bogus TC vortex for objective analysis with numerical weather prediction and for TC monitoring by TC forecasters.

In recent decades, the Dvorak technique (Dvorak 1975, 1984) has become a well-known standard for estimating TC intensity from TC cloud patterns observed in satellite infrared or visible imagery. Although this method provides reliable TC intensity estimates in many cases, several problems relating to the subjective and empirical approach by which it relates TC intensity to cloud patterns have been pointed out (e.g., Yoshida et al. 2011).

A warm core that forms with a positive temperature anomaly in relation to its environment above the surface at the center of a TC is a characteristic feature used to identify TC intensity. Intensification of the warm core due to latent heat release caused by convection causes MSLP values to decrease. In addition, adiabatic heating due to air subsidence inside the TC eye contributes to intensification of the warm core. The relationship between these temperature perturbations and MSLP is described by hydrostatic equilibrium theory. Since 1998, the Advanced Microwave Sounding Unit-A (AMSU-A) on board the NOAA and METOP polar orbital satellites have been available for the retrieval of warm core temperature profiles. Kidder et al. (2000) analyzed temperature profiles using AMSU-A brightness temperature (TB) data and applied the results to TC areas. A significant relationship was found between the maximum temperature anomaly corresponding to hurricane warm core intensity and MSLP.

To improve operational MSLP analysis, the Meteorological Research Institute (MRI) of JMA developed a new method for MSLP estimation using AMSU-A observation data (Oyama 2014), referred to here as the AMSU technique. The Regional Specialized Meteorological Center (RSMC) Tokyo - Typhoon Center began to use MSLP values estimated using the AMSU technique as reference data for JMA operational TC analysis and forecasting in the 2013 TC season. This paper gives an outline of the AMSU technique and highlights the quality and characteristics of the MSLP estimates it produces.

The paper consists of five sections. Following this introduction, Section 2 describes the data used for this study and MSLP estimation algorithm of the AMSU technique. Section 3 outlines the validation of MSLPs values estimated using the AMSU technique based on JMA best-track data for TCs observed from 2009 to 2011. In Section 4, characteristic aspects of MSLP estimates are explained with several TCs observed from 2009 to 2011 as examples. Finally, Section 5 provides a summary and future work.

2. Data and algorithm used for the AMSU technique

2.1 Data used in the study

In the AMSU technique, data on TC warm core intensity (defined as the maximum TB anomaly from TB values of AMSU-A 55-GHz band channels near the center of the TC) are used for MSLP estimation. Figure 1 shows the weighting functions of the AMSU-A 55-GHz band channels, and Table 1 (a) and (b) show the channel frequencies (Kidder et al. 2000). Table 1 (a) also shows the approximate pressure levels of the weighting function peaks displayed in Fig. 1. The weighting function for each

microwave channel of AMSU-A was computed from atmospheric transmittance data on the electromagnetic wave for each channel, which is controlled by the atmospheric gas density profile (Kidder and Vonder Haar 1995). Thus, the weighting function indicates the contribution of radiance from each atmospheric layer to the radiance observed by the satellite. In other words, the observed radiance mainly reflects the radiance from the pressure level of the weighting function peak. For example, the weighting function peaks for channels 6 and 7 (hereafter, for example, “channel 6” is abbreviated as “Ch6”) are located at around the pressure levels of 400 and 250 hPa, respectively. This difference in the weighting function peak level means that Ch6 can be used to observe microwave radiation from a lower height than Ch7.

Figure 2 shows the arrangement of AMSU-A Fields of View (FOVs) (Kidder et al. 2000). AMSU-A FOVs vary in size along the scan line, starting from 48 km near the nadir and increasing gradually to 150 km at the edges. The scan line orientation is approximately west-east. The variation of FOV sizes along the scan line is attributed to the cross-track scan observation of the NOAA and METOP satellites at 30 scan positions (Goldberg et al. 2001). For this study, geo-referenced and calibrated AMSU-A TB values (i.e., Level 1C data) obtained using ATOVS and AVHRR Pre-processing Package (AAPP) software (Atkinson 2011) were used. In addition, the limb adjustment technique was applied to correct the Level-1C TB values from each AMSU-A channel (Goldberg et al. 2001; Demuth et al. 2004) in order to reduce the effect of the atmospheric optical length on the TB fields.

For truth data, JMA best-track data (MSLP, TC central position and the shortest radius from the TC center of 30-knot surface winds at each analysis time, referred to here as “R30”) archived by the RSMC Tokyo - Typhoon Center were used (referred to here as “best-track data”).

Data from 22 TCs in 2008 were used to derive a regression equation for the relationship between warm core intensity and the MSLP of the best-track data (referred to here as “best-track MSLP”), and data on 57 TCs during 2009–2011 were used to validate the MSLP estimates. In this paper, TCs are referred to by their Asian names and by numbers indicating their order among the year’s TCs. For example, the 13th TC of 2008 was named Sinlaku, and is referred to as TC Sinlaku (0813). As the time interval of best-track data is generally six hours, the data were interpolated to the AMSU-A observation times when the MSLP estimates were validated. In addition, Dvorak analysis results (TC cloud patterns and the Current Intensity (CI) number) archived by the RSMC Tokyo - Typhoon Center were referred to in Section 4. JMA converts CI number to MSLP using a reference table proposed by Koba et al. (1990).

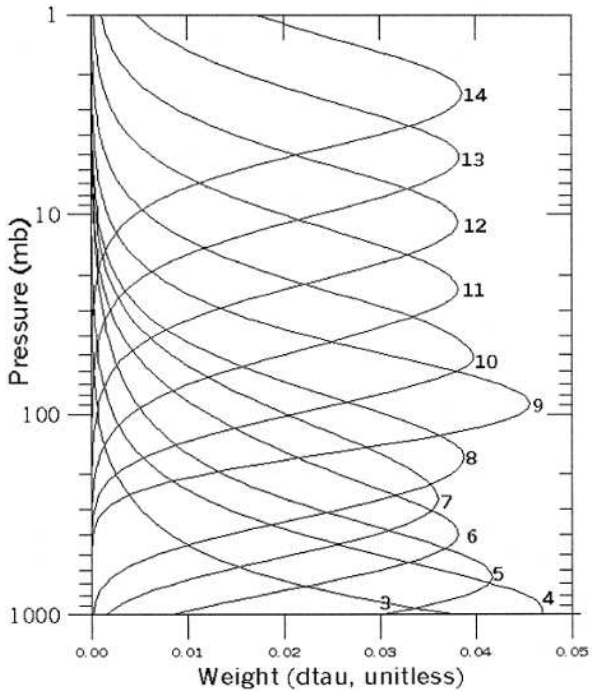

Fig. 1: Weighting functions of the AMSU-A 55-GHz band channels (Kidder et al. 2000). The number to the right of each line graph denotes the channel number.

Table 1: AMSU-A specifications (from Kidder et al. 2000). (a) Oxygen absorption band channel frequencies; (b) channels other than the oxygen absorption band. This table is adapted from Oyama (2014).

(a)

Channel No.	Frequency (GHz)	Approximate pressure level of weighting function peak
3	50.3	surface
4	52.8	900 hPa
5	53.6	600 hPa
6	54.4	400 hPa
7	54.9	250 hPa
8	55.5	180 hPa
9	57.2	90 hPa
10	57.29 ± 0.217	50 hPa
11	57.29 ± 0.322 ± 0.048	25 hPa
12	57.29 ± 0.322 ± 0.022	10 hPa
13	57.29 ± 0.322 ± 0.010	5 hPa
14	57.29 ± 0.322 ± 0.0045	2.5 hPa

(b)

Channel No.	Frequency (GHz)
1	23.8
2	31.4
15	89.0

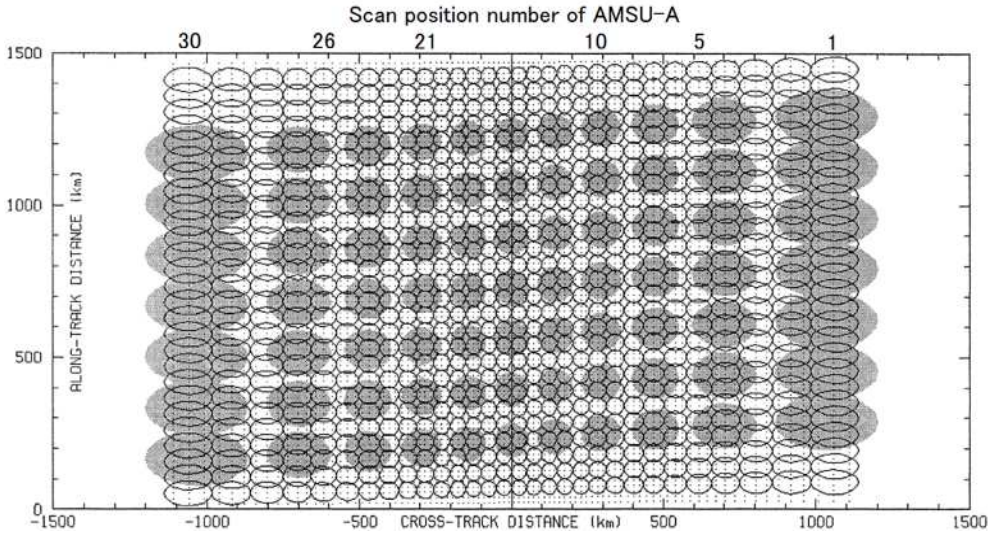

Fig. 2: FOVs of AMSU-A (open ellipses) and of the previous Microwave Sounding Unit (MSU) (filled gray ellipses) (Kidder et al. 2000). AMSU-A scan position numbers have been added at the top of the panel by the author.

2.2 MSLP estimation algorithm of the AMSU technique

The AMSU technique proposed by Oyama (2014) is based on hydrostatic equilibrium approximation, in which temperatures at altitudes between the surface and the top of the atmosphere are related to surface pressure. MSLP is related to vertically averaged temperatures at the TC center ($< T^{eye} >$) and in the surrounding environment ($< T^{env} >$) via approximation as shown in Eq. (1).

$$P_o^{eye} \cong P_0^{env}[1 - Constant \times (< T^{eye} > - < T^{env} >)], \quad (1)$$

where P_0^{eye} is the MSLP and P_0^{env} is the surface pressure in the surrounding environment. However, it is not realistic to apply the temperature profiles obtained from AMSU-A observations to Eq. (1) because AMSU-A TB values in the TC area are often attenuated due to microwave scattering caused by ice clouds and rain particles. This attenuation is large for channels whose weighting function peak level is near the surface (Knaff et al. 2000). Given these considerations, MSLP estimation in this study was based on upper tropospheric warm core intensity, defined as the maximum among the maximum TB anomaly values of AMSU-A Ch6, Ch7, and Ch8 within a radius of 200 km from the TC center. The warm core intensity is referred to here as “AMAX”, and the channel that finds AMAX values is referred to as “the AMAX channel”.

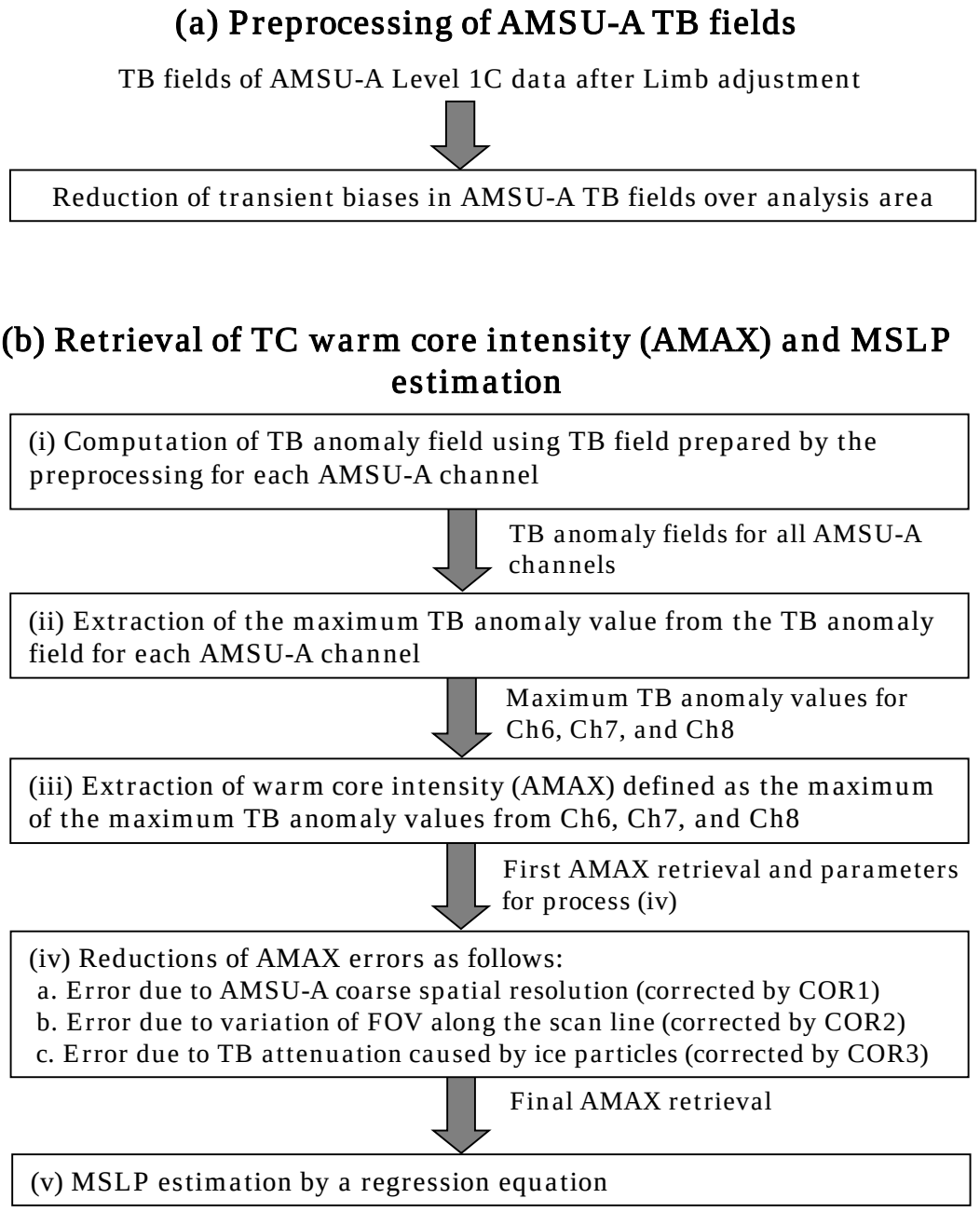

Fig. 3: Flow charts showing modules for (a) the preprocessing of AMSU-A TB fields, and (b) the retrieval of TC warm core intensity (AMAX) and MSLP estimation (Oyama 2014).

Figure 3 presents a flow chart of the algorithm for MSLP estimation from AMSU-A TB data. The algorithm consists of two modules: in module (a) the AMSU-A TB fields are preprocessed, and in module (b) AMAX is retrieved from the TB fields and used for MSLP estimation. The preprocessing module (a) calculations are performed before the module (b) calculations to prepare the TB fields for retrieving AMAX.

In module (b), the TB anomaly field representing the TC is computed by subtracting the environmental TB from the TB field. In this study, the average TB in the annulus between radii of 550 and 600 km from the TC center was defined as the default value of the environmental TB. If the radius of the positive TB perturbation corresponding to the warm core is greater than the default value, larger radii (up to 750 and 800 km) are adopted to define the annulus used to determine the environmental TB. The resulting TB anomaly field is used for the first AMAX retrieval. The final AMAX retrieval is obtained by applying correction to reduce the errors in the first AMAX retrieval due to AMSU-A weak points, that is, the coarse spatial resolution, FOV size variation along the scan line and TB attenuation caused by microwave scattering. The correction schemes to reduce the errors are described below.

a. Correction scheme 1 (COR1)

COR1 reduces the AMAX underestimation error caused by fact that the center of the FOV used to observe AMAX is not at the actual warm core center. AMAX is corrected using the distance between the AMAX position and the TC center (referred to here as *R1*), giving AMAX1, as follows:

$$\mathrm{AMAX1} = \mathrm{AMAX} + \mathrm{COEF1} \times R1, \tag{2}$$

where COEF1 depends on the parameter TBGRAD, which is the average horizontal TB gradient between the AMAX position and the neighbored FOV positions as shown in Fig. 4. *R1* can become substantially large in certain cases, such as when the determination error of TC center is large. To avoid AMAX1 overestimation caused by a large TC center determination error, AMAX was not corrected by Eq. (2) when *R1* was larger than (FOVSIZE + EYESIZE) / 2 (where FOVSIZE is the diameter of the FOV at the AMAX position, and EYESIZE is the typical TC eye diameter of 60 km).

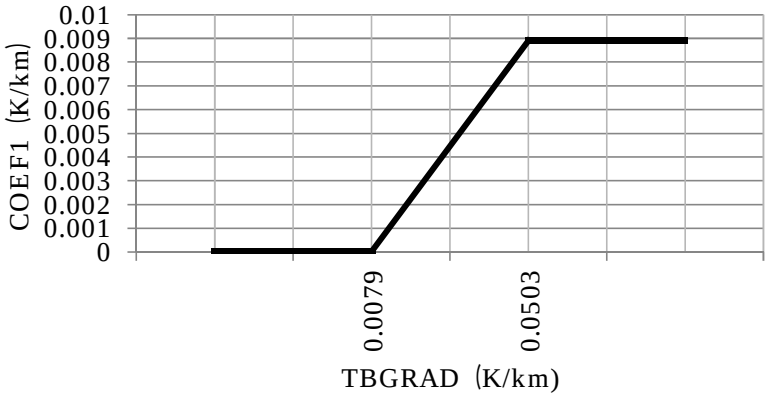

Fig. 4: COEF1 with reference to TBGRAD in Eq. (2) (Oyama 2014).

b. Correction scheme 2 (COR2)

COR2 reduces the effect on AMAX caused by FOV size variation along the scan line. It is used to evaluate the average AMAX underestimation due to FOV size at the AMAX position, which is then used to derive the corrected AMAX value, called AMAX2, as given by Eq. (3):

$$\mathrm{AMAX2} = \mathrm{AMAX1} + \mathrm{COEF2} \times (\mathrm{FOVSIZE} - \mathrm{FOVSIZE0}). \tag{3}$$

FOVSIZE0 in Eq. (3) is the diameter of FOV at nadir (=48 km). COEF2 was determined to be 4×10^{-3} K km^{-1} by evaluating the change in AMAX along the scan lines.

c. Correction scheme 3 (COR3)

COR3 reduces the underestimation error of AMAX caused by TB attenuation related to microwave scattering. To evaluate the magnitude of the microwave scattering, the Scattering Index over Water (SIW) (Grody et al. 2000) derived as Eq. (4) is introduced.

$$\mathrm{SIW} = -113.2 + \left(2.41 - 0.0049 \times \mathrm{TB(Ch1)}\right) \times \mathrm{TB(Ch1)} + 0.454 \times \mathrm{TB(Ch2)} - \mathrm{TB(Ch15)} \tag{4}$$

SIW increases with the magnitude of the microwave scattering up to about 85. The corrected AMAX, called AMAX3, is finally computed using SIW at the AMAX position as:

$$AMAX3 = AMAX2 + (SLOPE3 \times SIW + OFFSET3), \quad (5)$$

where the second term on the right-hand side is the average underestimation error of AMAX expected from SIW. The average underestimation error for SIW was evaluated in relation to the equivalent AMAX of the best-track MSLP for TCs where the influence of microwave scattering on AMAX is considered to be small (i.e., SIW < 20). SLOPE3 and OFFSET3 were determined for each AMAX channel by the least-squares method as shown in Table 2.

COR1, COR2, and COR3 were derived using 365 AMAX observations at scan positions from position No.5 to No.26 (see Fig. 2) for 22 TCs in 2008 because AMAX retrieval near the edges of the scan lines may be inaccurate. Finally, MSLP is estimated using the corrected AMAX obtained by Eq. (5) (i.e., AMAX3) as:

$$MSLP = SLOPE \times AMAX + OFFSET. \quad (6)$$

The parameters SLOPE and OFFSET in Eq. (6) were derived by relating the corrected AMAX value to the best-track MSLPs by the least-squares method using AMSU-A observations for the 22 TCs in 2008. To take account of the properties of each AMSU-A channel with regard to warm core observations, SLOPE and OFFSET were derived separately for each AMAX channel as Table 3. Eventually, 245 AMAXs with small SIW (<20) at scan positions from position No.7 to No.24 (see Fig. 2) were used for deriving SLOPE and OFFSET.

Table 2: SLOPE3 and OFFSET3 in Eq. (5) (Oyama 2014).

AMAX channel	SLOPE3	OFFSET3
Ch6	0.0246	-0.0143
Ch7	0.0128	-0.1543
Ch8	0.0235	-0.0965

Table 3: SLOPE and OFFSET in Eq. (6) (Oyama 2014).

AMAX channel	SLOPE	OFFSET
Ch6	-10.63	1012.05
Ch7	-14.36	1010.96
Ch8	-14.26	1013.55

3. Validation of AMSU MSLP for TCs observed from 2009 to 2011

Validation of MSLPs estimated by using the AMSU technique (referred to here as "AMSU MSLP") with reference to best-track MSLP was performed for TCs observed from 2009 to 2011. The results show that the correlation between AMSU MSLPs and best-track MSLPs for 1,029 TC observations was high at 0.89 (Fig. 5). The root mean square error (RMSE) and bias of AMSU MSLPs with reference to the best-track MSLPs were 10.1 and 0.3 hPa, respectively. The MSLP estimation error was within ±5 hPa for 51.0% of all observations and within ±10 hPa for 79.3% of the total. However, some AMSU MSLPs were substantially higher than best-track MSLP when best-track MSLPs were between 930 hPa and 970 hPa (Fig. 5). Oyama (2014) suggested that they may be attributed to strong microwave scattering near TC center and/or a small warm core compared to the spatial resolution of AMSU-A observation.

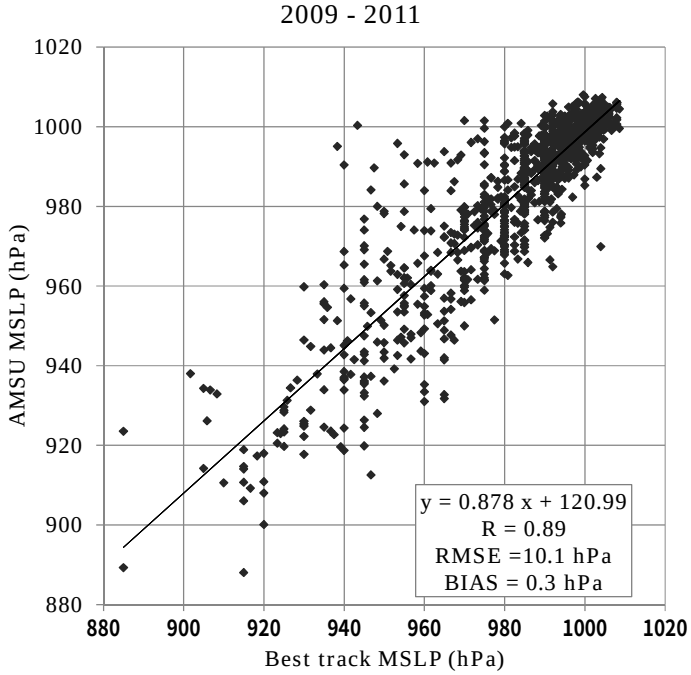

Fig. 5: Scatter plots between AMSU MSLPs and best-track MSLPs for 1,029 observations of TCs seen from 2009 to 2011 (Oyama 2014). *R* is the correlation coefficient between AMSU MSLP values and the best-track MSLP values.

4 Characteristics of AMSU MSLP values

Oyama (2014) highlighted the characteristic aspects of AMSU MSLP values relating to TC cloud patterns and TC size as defined by R30:

(i) The quality of AMSU MSLP with reference to best-track data tends to be better for large TCs than that for compact ones.

(ii) The quality of AMSU MSLP with reference to best-track data tends to be better than that of MSLP estimated using the Dvorak technique (referred to here as "Dvorak MSLP") at least when the TC is not compact and the TC cloud pattern is the Curved Band pattern or the Shear / Low level Cloud Vortex (LCV) pattern.

(iii) AMSU MSLPs tend to be higher than best-track MSLPs when microwave scattering caused by ice particles near TC center is too large or TC size is small.

In the rest of this section, the characteristics of AMSU MSLPs in terms of the above points (i) – (iii) are outlined in relation to several TCs observed from 2009 to 2011 by comparing AMSU MSLPs with the best-track MSLPs and Dvorak MSLPs. It should be noted that the best-track MSLP depends on the Dvorak MSLP. This tends to be particularly true for regions where in situ data are sparse. For discussion of TC size, the R30 of particular TCs and the average R30 for TCs observed from 2000 to 2011 (Table 4) are used.

Table 4: Average R30 between 2000 and 2011 for 11 MSLP classes based on best-track data (Oyama 2014).

Best track MSLP (hPa)	Average R30 (km)	Number of best track data
MSLP < 910	366.7	11
910 ≦ MSLP < 920	400.6	69
920 ≦ MSLP < 930	397.7	164
930 ≦ MSLP < 940	394.6	308
940 ≦ MSLP < 950	376.0	591
950 ≦ MSLP < 960	354.9	698
960 ≦ MSLP < 970	329.6	751
970 ≦ MSLP < 980	311.4	945
980 ≦ MSLP < 990	261.8	1295
990 ≦ MSLP < 1000	197.6	1746
1000 ≦ MSLP	153.6	210

TC Meari (1105) was a case in which AMSU MSLP values better matched best-track MSLP values than Dvorak MSLP values. Figure 6 shows a time-series representation of AMSU MSLP, Dvorak MSLP, best-track MSLP, and R30 values for this TC. TC Meari

was relatively weak with an MSLP of just 975 hPa even at its mature stage (Fig. 6). It was accompanied by two characteristic features that may explain why the quality of AMSU MSLP was higher than that of Dvorak MSLP. First, the R30 of TC Meari was much larger than the average R30 during its lifecycle. Second, the cloud patterns determined by JMA were the Curved band pattern (from 00 to 11 UTC on 24 June and from 00 to 09 UTC on 25 June) and Shear/LCV pattern (from 18 UTC on 25 June to 21 UTC on 26 June). It should be noted that TC Meari was not accompanied by active cumulonimbus clouds and large SIW near its center when the AMSU MSLP was substantially closer to the best-track MSLP than the Dvorak MSLP (Figs. 7d-e).

TC Chaba (1014) was another case in which AMSU MSLP well matched best-track MSLP, but this one was more intense than TC Meari. JMA determined the cloud patterns of TC Chaba as the Cb cluster pattern, the Curved band pattern, the Eye pattern, the Central Dense Overcast (CDO) pattern and the Shear / LCV pattern depending on the life stage. The AMSU MSLP and Dvorak MSLP values were nearly equal to the best-track MSLP values throughout the TC's lifetime (Fig. 8). The good quality of AMSU MSLP data for TC Chaba was probably due to the non-compact warm core as resolved by AMSU-A instrument. In fact, the R30 of TC Chaba was comparable to the average R30 during its lifetime (Fig. 8 and Table 4). It should also be noted that the difference between AMSU MSLP and best-track MSLP was small even though TC Chaba exhibited large SIW values near its center (Fig. 9d), which had a small TC eye seen in MTSAT infrared TB imagery (Fig. 9e). This situation suggested that COR3 worked well for this TC.

TC Mirinae (0921) had the worst MSLP estimations from the AMSU technique for the period from 2009 to 2011. As seen in Fig. 10, AMSU MSLP was much higher than best-track MSLP and Dvorak MSLP, particularly from 28 October to 29 October during the mature stage. The positive TB anomalies near the TC center for Ch6, Ch7 and Ch8, which correspond to the temperature perturbations of the warm core, were small during this period (Figs. 11a-c). The influence of TB attenuation caused by microwave scattering on AMSU MSLP was possibly small at that time because SIW values near the TC center were small (Fig. 11d). A feature that explains the significantly higher AMSU MSLP than the best-track MSLP is the compactness of TC Mirinae (see R30 in Fig. 10 and Fig. 11e). Thus, it can be said that the warm core of TC Mirinae was too small to be observed using AMSU-A instrument.

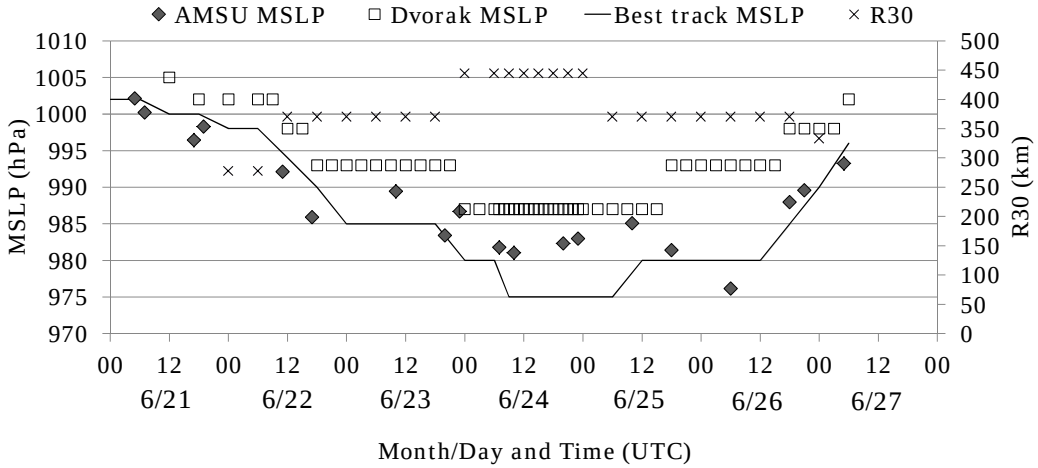

Fig. 6: Time series of AMSU MSLP (gray diamonds), Dvorak MSLP (white squares), best-track MSLP (line graph), and R30 values (cross plots) for TC Meari (1105).

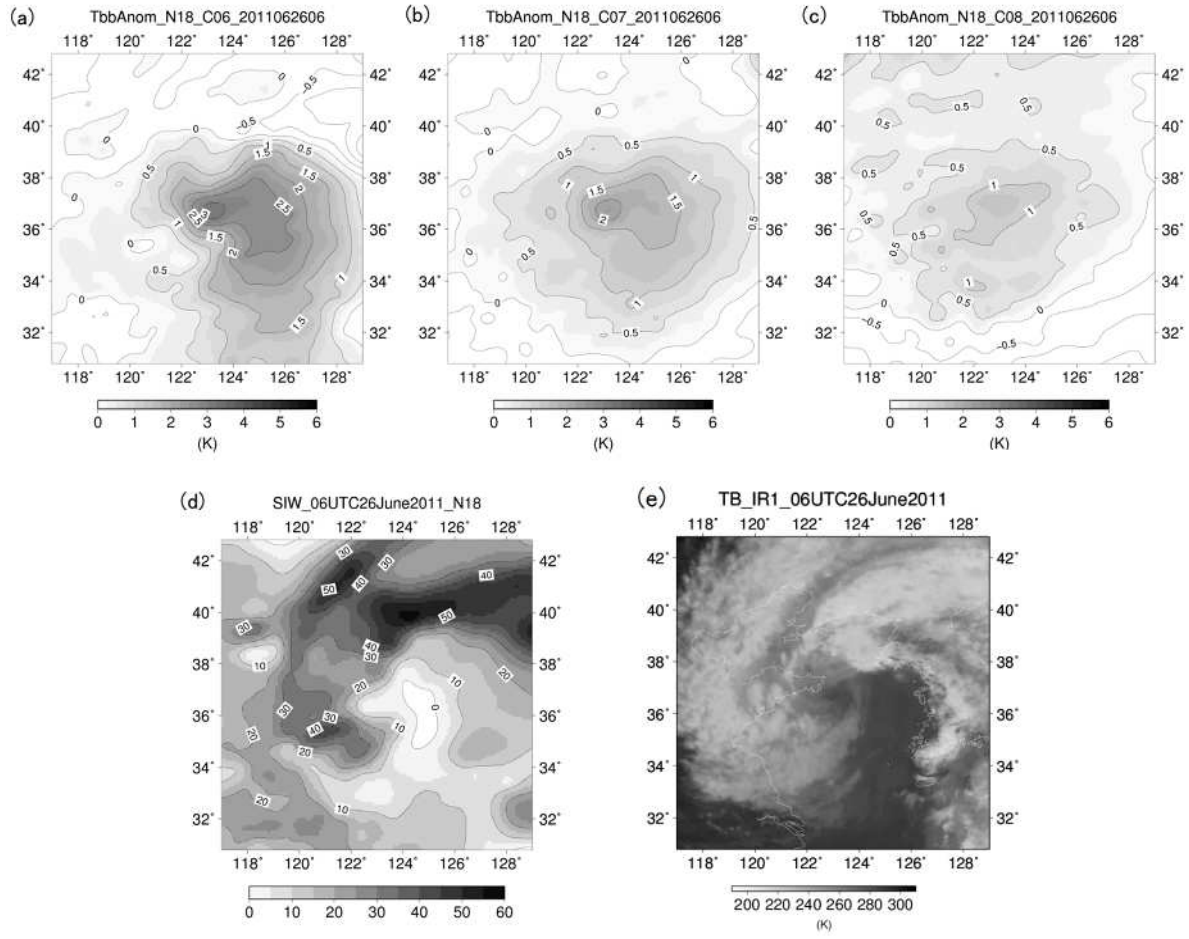

Fig. 7: Spatial distributions of AMSU-A TB anomalies for (a) Ch6, (b) Ch7, and (c) Ch8 along with distributions of (d) SIW and (e) MTSAT infrared (10.8 μm) TB values in an area covering 12° longitude × 12° latitude centered on TC Meari (1105) at 06 UTC on 26 June 2011 during the decay stage. AMAX was observed by Ch6.

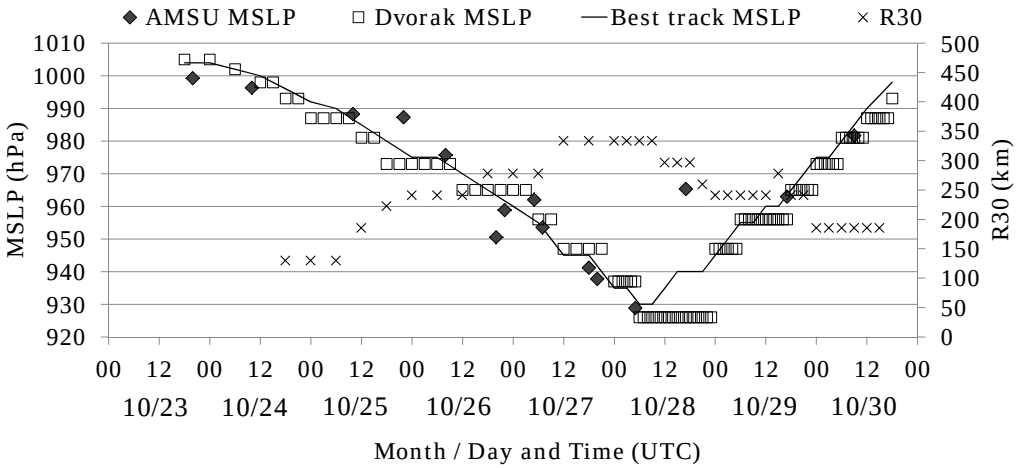

Fig. 8: Same figure as Fig. 6, but for TC Chaba (1014).

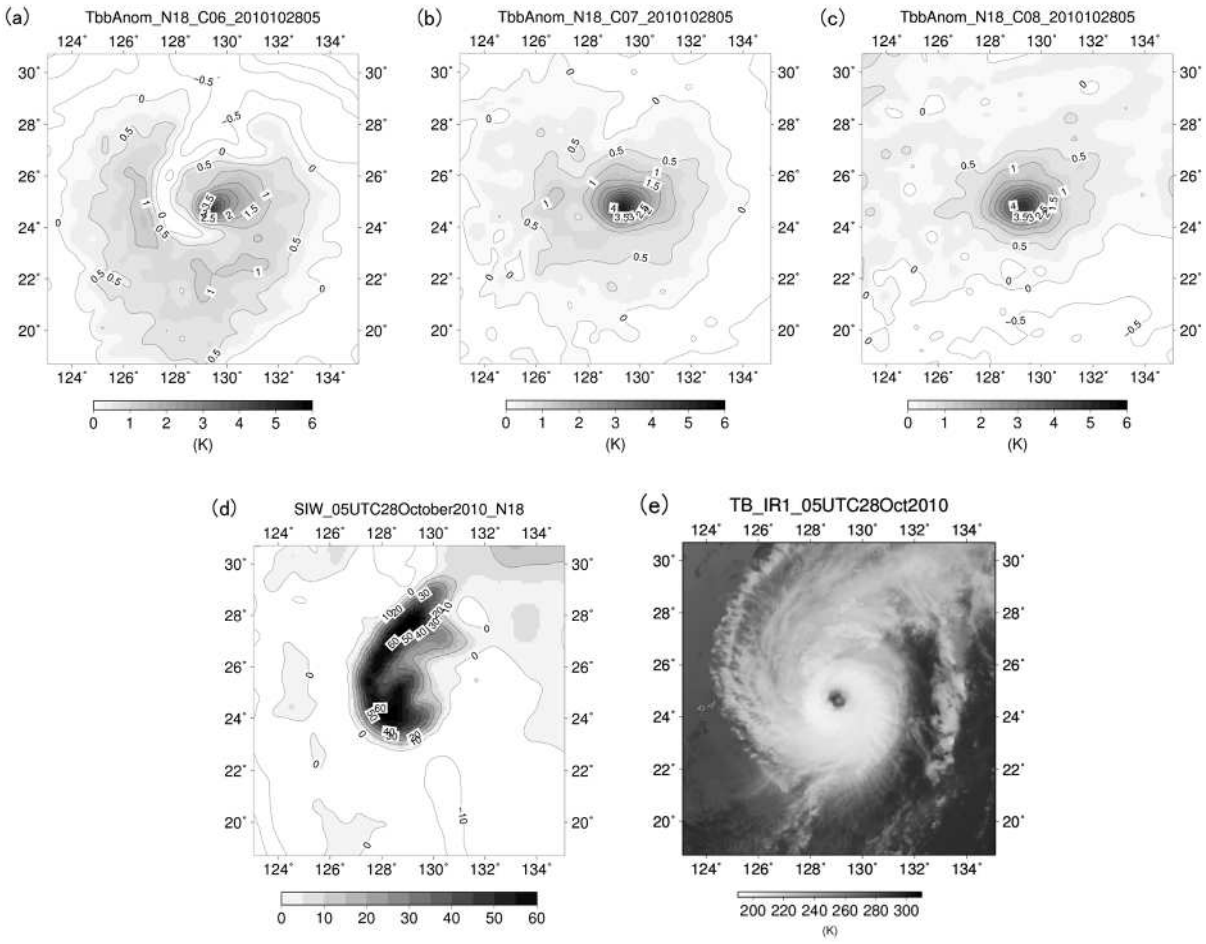

Fig. 9: Same figure as Fig. 7, but for TC Chaba (1014) at 05 UTC on 28 October 2010 in the mature stage. AMAX was observed by Ch7.

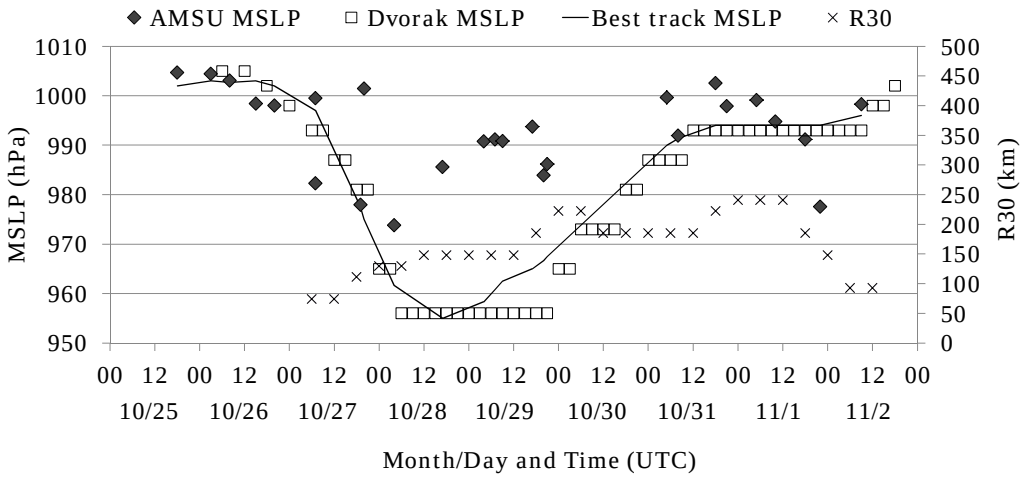

Fig. 10: Same figure as Fig. 6 but for TC Mirinae (0921).

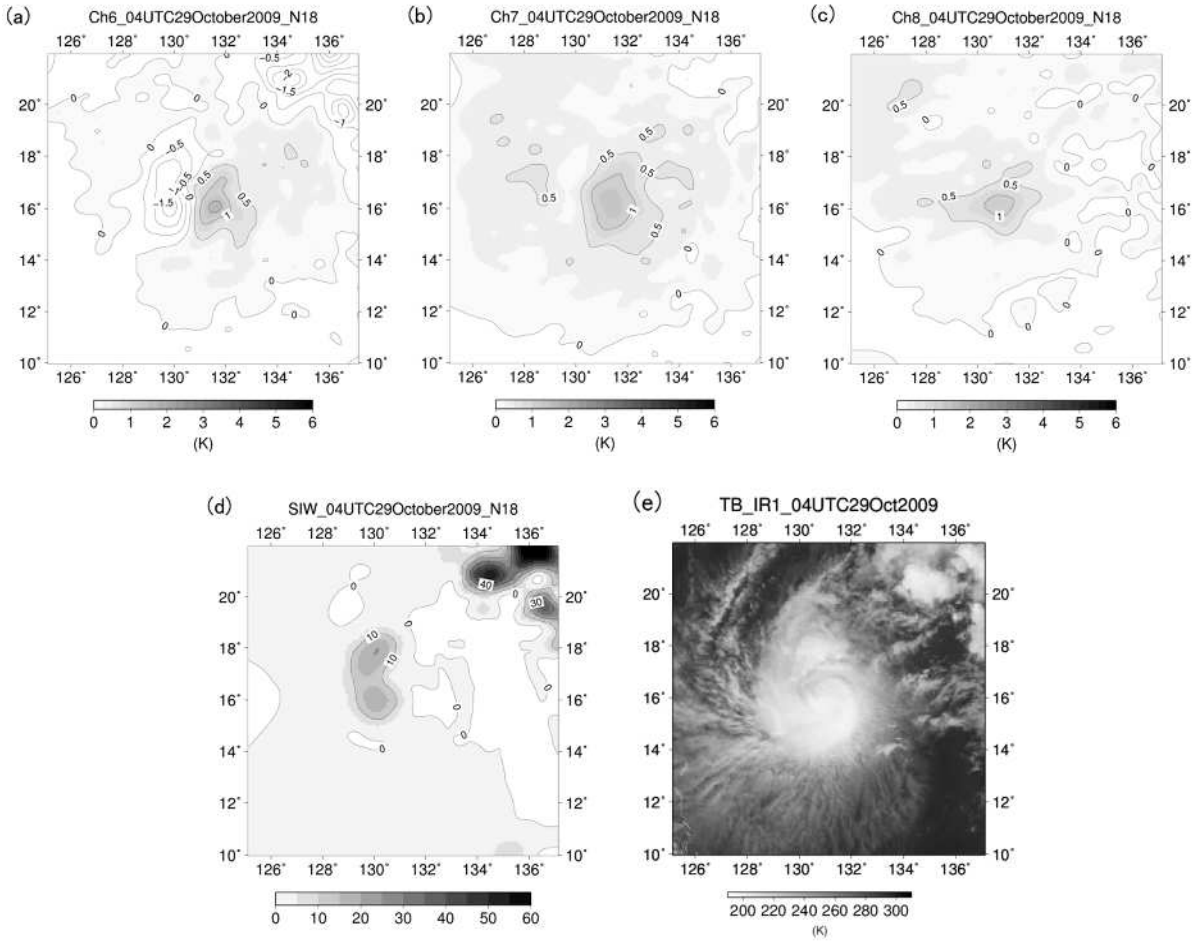

Fig. 11: Same figure as Fig. 7 but for TC Mirinae (0921) at 04 UTC on 29 October 2009 during the mature stage. AMAX was observed by Ch7.

5. Conclusion

To improve operational MSLP analysis, MRI/JMA developed a new MSLP estimation method based on TC warm core intensity data retrieved from AMSU-A 55-GHz band TB values. This approach involves the use of regression between TC warm core intensity (defined as the maximum TB anomaly) and best-track MSLP values for the 2008 TC season. The possible errors of the maximum TB anomaly due to AMSU-A weak points (i.e., coarse spatial resolution, FOV size variation along the scan line and TB attenuation caused by microwave scattering) were corrected using the schemes developed in this study.

The RMSE and bias of AMSU MSLP values with reference to best-track MSLP values for 57 TCs observed from 2009 to 2011 were 10.1 and 0.3 hPa, respectively. The MSLP estimation error was within ±5 hPa for 51.0% of all observations and within ±10 hPa for 79.3% of the total. The characteristics of AMSU MSLPs relating to TC cloud pattern and TC size were also elucidated in relation to TC Meari (1105), TC Chaba (1014), and TC Mirinae (0921).

It is important to use AMSU MSLPs appropriately with Dvorak MSLPs and other MSLP estimates in operational MSLP analysis (Velden et al. 2007). The characteristics of AMSU MSLP clarified as a result of this study are expected to contribute to the optimal use of AMSU MSLP for the analysis.

References

Atkinson, N., 2011: AAPP Overview, Satellite Application Facility for Numerical Weather Prediction. *NWPSAF-MO-UD-004, Version 7.0 (available at http://research.metoffice.gov.uk/research/interproj/nwpsaf/aapp/)*

Demuth, J. L., M. DeMaria, J. A. Knaff, and T. H. Vonder Haar, 2004: Evaluation of Advanced Microwave Sounding Unit tropical-cyclone intensity and size estimation algorithms. *J. Appl. Meteor.*, **43**, 282-296.

Dvorak, V. F., 1975: Tropical cyclone intensity analysis and forecasting from satellite imagery. *Mon. Wea. Rev.*, **103**, 420-430.

Dvorak, V. F., 1984: Tropical cyclone intensity analysis using satellite data. *NOAA Technical Report NESDIS*, **11**, 47pp.

Goldberg, M. D., D. S. Crosby, and L. Zhou, 2001: The limb adjustment of AMSU-A observations, Methodology and Validation. *J. Appl. Meteor.*, **40**, 70-83.

Grody, N., F. Weng, and R. Ferraro, 2000: Application of AMSU for obtaining

hydrological parameters. *Microwave Radiometry and Remote Sensing of the Earth's Surface and Atmosphere. P. Pampaloni and S. Paloscia (Eds)*, 339-351.

Knaff J. A., R. M. Zehr, M. D. Goldberg, and S.Q. Kidder, 2000: An example of temperature structure differences in two cyclone systems derived from the Advanced Microwave Sounder Unit. *Wea. Forecasting*, **15**, 476-483.

Kidder, S. Q. and Thomas H. Vonder Haar, 1995: *Satellite Meteorology, An Introduction*. *Academic Press,* 183-189.

Kidder, S. Q., M. D. Goldberg, R. M. Zehr, M. DeMaria, J. F. W. Purdom, C. S. Velden, N. C. Grody, and S. J. Kusselson, 2000: Satellite analysis of tropical cyclones using the Advanced Microwave Sounding Unit (AMSU). *Bull. Amer. Meteor. Soc.*, **81**, 1241-1259.

Koba, H., T. Hagiwara, S. Osano, and S. Akashi, 1990: Relationship between the CI-number and central pressure and maximum wind speed in typhoons. *J. Meteor. Res.,* **42**, 59–67 (in Japanese).

Oyama, R., 2014: Estimation of tropical cyclone central pressure from warm core intensity observed by the Advanced Microwave Sounding Unit-A (AMSU-A), *Pap. Meteor. Geophys.*, **65**, 35-56.

Velden, C., D. Herndon, J. Kossin, J. Hawkins, and M. DeMaria, 2007: Consensus Estimates of Tropical Cyclone (TC) Intensity using Integrated Multispectral (IR and MW) Satellite Observations, Joint 2007 EUMETSAT Meteorological Satellite & 15th AMS Satellite Meteorology and Oceanography conference (*http://www.ssec.wisc.edu/meetings/jointsatmet2007/pdf/velden_satcon.pdf*)

Yoshida, S., M. Sakai, A. Shouji, M. Hirohata, and A. Shimizu, 2011: Estimation of tropical cyclone intensity using Aqua/AMSR-E Data, *RSMC Tokyo – Typhoon Center technical review*, **13**, 1-36.